Original Scientific Article • DOI: 10.2478/rmzmag-2021-0006

Received: October 21, 2021
Accepted: November 26, 2021

Determination of material quality by methods of thermal analysis

Ugotavljanje kakovosti materiala z metodami termične analize

Maja Vončina[1,*], Gregor Hvala[1], Jožef Medved[1], Borut Žužek[2], Mitja Petrič[1]

[1]University of Ljubljana, Faculty of Natural Sciences and Engineering, Department of Materials and Metallurgy, Ljubljana, Slovenia

[2]Institute of Metals and Technology, Lepi pot 11, 1000 Ljubljana, Slovenia

*Corresponding author: E-mail: maja.voncina@ntf.uni-lj.si

Abstract in English

Cast aluminium alloys are commonly used in the automotive industry for casting applications. There are both primary and secondary/recycled aluminium alloys in the market, which differ in price and quality. In this study, the effect of alloy quality on solidification, microstructure and mechanical properties was investigated. The comparison of properties was carried out in the as-cast condition and in the heat-treated condition. The influence of alloy quality on solidification was analysed by simple thermal analysis and differential scanning calorimetry, and thermodynamic simulations. The basic mechanical properties analysed were tensile strength, yield strength, elongation, and hardness. The microstructural differences were analysed using a light microscope. The Mn:Fe ratio, which is strongly influenced by the alloy quality, was found to have a pronounced effect on the mechanical properties, while magnesium together with silicon hardens the aluminium matrix during heat treatment, which significantly increases the mechanical properties.
This research proved that thermal analysis methods can give us a necessary and important indication of the quality of the alloys used.

Keywords: Alloy quality, casting alloys, thermal analysis, solidification, microstructure, mechanical properties

Povzetek

Aluminijeve zlitine se pogosto uporabljajo v avtomobilski industriji pri vlivanju. Na trgu obstajajo primarne in sekundarne/reciklirane aluminijeve zlitine, ki se razlikujejo po ceni in kakovosti. V tej študiji je bil raziskan vpliv kakovosti zlitine na strjevanje, mikrostrukturo in mehanske lastnosti. Primerjava lastnosti je bila narejena v litem in v toplotno obdelanem stanju. Vpliv kakovosti zlitine na strjevanje smo analizirali z enostavno termično analizo in diferenčno vrstično kalorimetrijo ter termodinamičnimi simulacijami. Analizirane so bile osnovne mehanske lastnosti, kot so natezna trdnost, meja tečenja, raztezek in trdota. Mikrostrukturne razlike smo analizirali z optičnim mikroskopom. Dokazano je, da razmerje Mn:Fe, na katerega močno vpliva kakovost zlitine, izrazito vpliva na mehanske lastnosti, medtem ko magnezij skupaj s silicijem med toplotno obdelavo utrjuje aluminijasto matrico, kar tudi bistveno poveča mehanske lastnosti.
V tej raziskavi je bilo dokazano, da nam lahko metode termične analize dajo potreben in pomemben podatek o kakovosti uporabljenih zlitin.

Ključne besede: kakovost zlitin, livarske zlitine, termična analiza, strjevanje, mikrostruktura, mehanske lastnosti

Introduction

One of the few disadvantages of aluminium is its expensive and energy-intensive extraction. It is mainly extracted from bauxite ore by the Bayer process. This produces alumina (Al_2O_3), from which technically pure aluminium is later extracted by electrolysis. An alternative to this extraction method is secondary extraction, that is, recycling, which requires only about 10% of the energy needed to produce one tonne of primary aluminium. The disadvantage of recycling

is the slightly higher content of some elements, the removal of which is extremely difficult or inadvisable. One such element is iron, which is otherwise required in the die casting of aluminium alloys because it prevents the castings from soldering to the tool. However, too much iron can deteriorate the alloy's mechanical properties.

The addition of magnesium to Al-Si alloys is the basis for the group of alloys characterized by exceptional castability and excellent mechanical properties after heat treatment. They are corrosion resistant and thermal expansion is low. Magnesium is added to binary alloys to improve the properties after heat treatment T6, which is characteristic of this type of alloy, through the mechanism of precipitation hardening. The heat treatment consists of solution annealing, quenching, and artificial aging, during which the hardening intermetallic phase Mg_2Si precipitates. The mechanical properties can be further improved by the addition of manganese and beryllium, which affect the morphology of the iron-based phases, improving the strength properties and ductility [1, 2]. The best effect of magnesium addition is seen at a content between 0.2 and 0.6% by weight, very rarely exceeding 1% by weight. The lower limit is determined by a sufficient amount for precipitation of the Mg_2Si phase, so that the effect on the mechanical properties is noticeable. The upper limit is determined by a still satisfactory plasticity; there should not be too much Mg_2Si phase in the microstructure. The magnesium content has a great influence on aging, so that the permissible limits in the individual alloys are very narrow. They also depend very much on the other alloying elements and the expected aging regime of the alloy [3, 4].

Solidification of AlSi10Mg and AlSi10Mg(Fe) alloys depends largely on the cooling rate and alloying elements, and usually begins in the temperature range between 550 °C and 600 °C. Solidification of this type proceeds as follows: First, the primary aluminium α-Al crystals solidify at T_L. Further eutectic (α-Al + β-Si) is formed, meanwhile, the remaining melt is enriched with the other elements, leading to the formation of different intermetallic phases. The first to solidify are the Fe-phases α-$Al_{15}(Fe,Mn)_3Si_2$ and β-Al_5FeSi, and among the latter, the Mg-phase Mg_2Si solidifies. The proportion and ratio of these phases depend on the ratio of manganese and iron in the alloy [5, 6, 7].

Strength properties increase significantly after heat treatment compared to as-cast condition. The elongation at yield strength decreases. Compared to alloys with different iron contents, the solidification rate has a great influence. The hardness is higher in the secondary alloy due to the higher iron content [3, 4, 8, 9].

Inferior alloys may contain up to twice as much iron. Two Fe-phases form in cast aluminium alloys, namely, α-$Al_{15}(Fe,Mn)_3Si_2$ and β-Al_5FeSi. The former is more desirable due to its rounded shape in the microstructure, as it does not adversely affect the mechanical properties like β-Al_5FeSi. Therefore, manganese is added to the alloys to convert the needles of the β-Fe_5FeSi phase to the α-$Al_{15}(Fe,Mn)_3Si_2$ phase. The optimum Mn:Fe ratio in the alloys was found to be about 0.5 [10].

Materials and methods

Based on the chemical composition of the studied alloys, listed in Table 1, a simulation of Scheil's thermodynamic non-equilibrium solidification was performed, using Thermo-Calc software and the TCAL6 database. Alloy AlSi10Mg is marked as 239, with better and purer quality, and alloy AlSi10Mg(Fe) as 239D, of inferior quality.

To characterize the solidification path of two alloys under investigation, the samples were melted in an induction furnace in a steel crucible coated with BN-foundry coating. The experimental alloy was preheated to 700 °C. After completion of the melting process, the experimental samples were then cast at a temperature of 700 °C in a Croning measuring cell, where the cooling rate was ~ 7 K/s and cooling curves were recorded. To characterize the accurate solidification of the test alloys, corresponding initial derivatives were obtained from the cooling curves. At the same time, the melt was also poured into a square steel mould (Figure 1), from which four specimens were obtained for the tensile tests.

Differential scanning calorimetry (DSC) analyses were also carried out to determine the

Table 1: *Chemical composition of the alloys investigated in % by weight.*

Sample	Si	Fe	Cu	Mn	Mg	Ni	
239	10.398	0.3548	0.005	0.2654	0.5513	0.0038	
239D	10.439	0.8788	0.0229	0.3092	0.4459	0.0062	
Sample	Zn	Pb	Sn	Ti	Sr	Al	Mn:Fe
239	0.0039	0.001	0.0003	0.0983	0.0369	rest	0.748
239D	0.0167	0.001	0.0004	0.0253	0.0015	rest	0.352

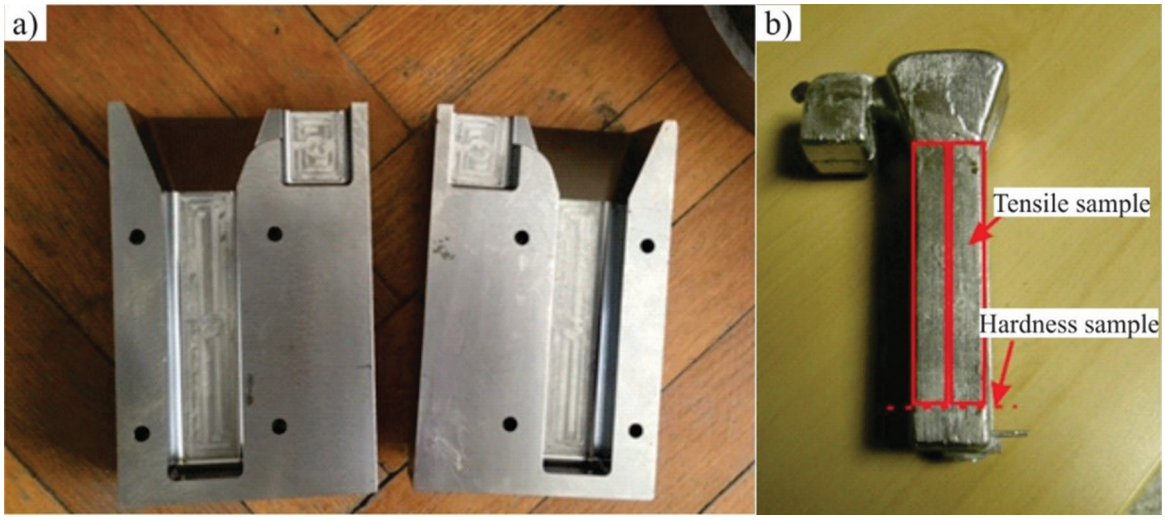

Figure 1: *(a) Steel mould with a square profile; (b) Casting obtained from the steel mould for tensile specimens.*

temperature changes and thermal effects occurring during heating / melting and cooling / solidification of the alloys studied. The experiments were carried out using a STA Jupiter 449C instrument from Netzsch by placing two identical corundum crucibles on the platinum sensor. The sample under investigation was placed in one crucible and an (inert) reference sample in the other. The system was heated to 720 °C in a furnace according to the preprogrammed temperature programme. It was kept at this temperature for 10 minutes. The heating and cooling phases were performed at a constant rate of 10 K / min. The test was performed in a protective atmosphere of Ar 6.0. During the measurement, the instrument recorded the temperature, the temperature difference between the tested sample and the reference sample, and the time. DSC analysis was performed on cast samples taken from the centre of the casting from Croning measurement cell [11]. The samples were turned to a diameter of 4.5 mm and a height of 4 mm and inserted into the instrument where the analysis was performed. After the measurements, the heating and cooling curves of the DSC were recorded, while the characteristic temperatures were determined from the heating and cooling curves of the DSC.

Specimens for microstructure investigations were prepared metallographically from the center of the casting from the Croning measuring cell [11] and photographed with a BX61 light microscope to analyze the effect of alloy quality on the formation and distribution of microstructural constituents.

Specimens of B 6 x 30 mm type were used for the tensile test, prepared according to DIN 50125: 2016-12. Four specimens of each test alloy were prepared in as-cast and T6 heat-treated condition. Tensile tests were carried out on INSTRON 8802 apparatus in accordance with SIST EN ISO 6892-1:2020 A224 standard.

To analyse the hardness of two grades of alloy in the as-cast and heat-treated condition, the instrument NEXUS 7500 was used and the measurements were made in accordance with the standard SIST EN ISO 6506 - 1: 2014. A tungsten carbide ball with an HBW of 2.5 / 62.5 was used. Hardness measurements were carried out on specimens from a square-profile steel mould.

Results and discussion

Figure 1a shows the calculated cooling curve of sample 239 and Figure 2b shows the calculated cooling curve of sample 239D, where the dashed line indicates the equilibrium solidification. The results show that in sample 239 both Fe-phases solidify after the primary α-Al crystals and eutectic (α-Al + β-Si). It does not end with the Fe-phase β-Al_5FeSi; the phases π-$Al_8Si_6Mg_3Fe$ and Mg_2Si also solidify from the melt. The main difference between the investigated alloys is that at the alloy 239D the solidification of both Fe-phases occurs before the solidification of eutectic (α-Al + β-Si), whereas also the amount of those phases is much higher, respectively. The solidus temperature T_S is 554.7 °C for sample 239 and 555.1 °C for sample 239D.

The main difference between the samples / alloys in solidification, calculated with the Thermo-Calc program, is seen in the sonification path and proportions of each phase (Table 2). The calculated amount of Fe-phase α-$Al_{15}(Fe,Mn)_3Si_2$ in sample 239D is about twice that in sample 239, and an even greater difference occurs for the β-Al_5FeSi phase; it is up to 150% higher than in sample 239.

The cooling curves in Figure 3 show that the T_L in sample 239 is higher and the solidification interval is wider, which is consistent with Scheil's non-equilibrium solidification curve. This is followed by the solidification of the Fe-phases, the onset of which is indicated by T_1. This was determined from the derivative where the cooling rate is high, followed by a drop in the cooling rate due to the release of latent heat. This is followed by solidification of the eutectic with Fe-phases, namely α-$Al_{15}(Fe,Mn)_3Si_2$ and / or β-Al_5FeSi. Undercooling after the onset of eutectic solidification is illustrated by the temperature $T_{E/min}$, latent heat is released by the solidification and the temperature increases to $T_{E/max}$. The solidification proceeds in the same way until the temperature T_2, which was observed only for sample 239. Using calculations with Thermo-Calc, the eutectic solidification of the π-$Al_8Si_6Mg_3Fe$ phase can be predicted. The point T_3 represents the beginning of the solidification of the Mg_2Si eutectic phase. The final solidification temperatures (solidus temperatures) are much lower than those theoretically determined by the Scheil simulation of non-equilibrium solidification.

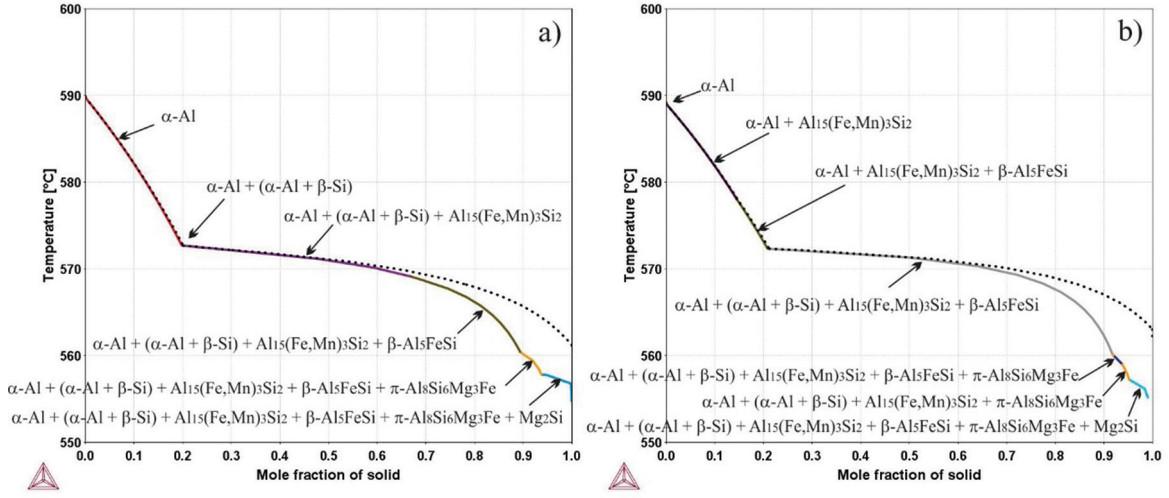

Figure 2: *The Scheil cooling curve of the non-equilibrium solidification of (a) sample 239 and (b) sample 239D.*

The results of the DSC analysis are shown in Figure 4 and show both the heating (green) and cooling (blue) curves for both samples tested. In both figures, the first inflexion point is at about 220 °C and can be associated with the precipitation of the Q-$Al_5Cu_2Mg_8Si_6$ or Mg_2Si phase; a later point is not possible due to the very low copper content in the samples (239: 0.005 wt%; 239D: 0.0229 wt%). The second inflexion point represents T_S (239: 552.2 °C; 239D: 551.2 °C) and illustrates the onset of eutectic melting (α-Al + β-Si) with the Mg_2Si phase present. According to Thermo-Calc calculations, the next characteristic point (239: 565.5 °C; 239D: 563.7 °C) defines the melting of the eutectic (α-Al + β-Si) and the last characteristic temperature (239: 608.1 °C; 239D: 605.0 °C) represents the melting of the primary α-Al dendrites. On the cooling curves (blue), the first characteristic point is T_L (239: 575.5 °C; 239D: 569.4 °C), where the solidification of the primary α-Al dendrites begin. According to Thermo-Calc calculations, the next inflexion point is the solidification temperature of the eutectic (α-Al + β-Si) and the last one is the solidification of the eutectic (α-Al + β-Si + Mg_2Si) (239: 522.1 °C; 239D: 521.8 °C). In sample 239D, another inflexion point occurs at 544.3 °C, which most likely represents the eutectic solidification of the Fe-phases.

Table 2: *The proportions of phase formed during the solidification.*

Phase / Sample	239	239D
α-Al	87.00	85.20
β-Si (eutectic)	9.91	9.74
α-$Al_{15}(Fe,Mn)_3Si_2$	0.89	1.03
β-Al_5FeSi	1.31	3.26
Mg_2Si	0.86	0.65
Q-$Al_5Cu_2Mg_8Si_6$	0.02	0.11

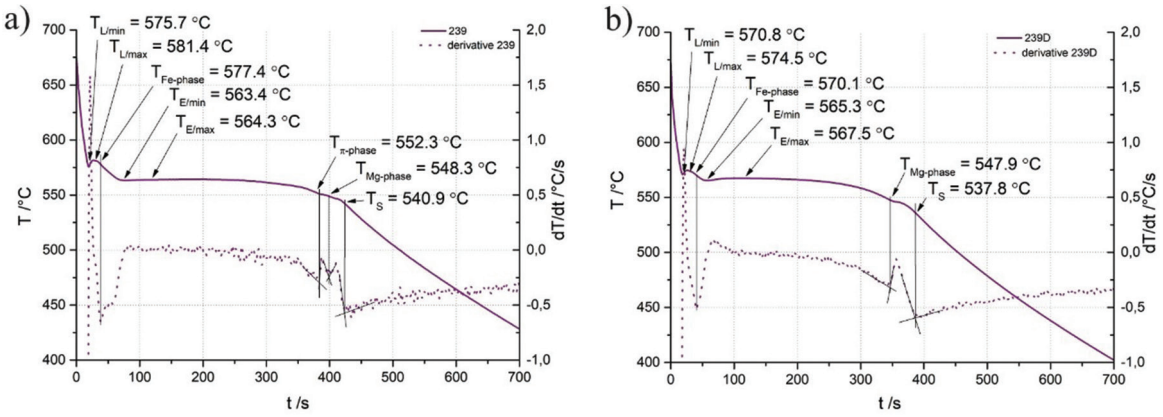

Figure 3: *The cooling curve and corresponding derivative of (a) sample 239 and (b) sample 239D.*

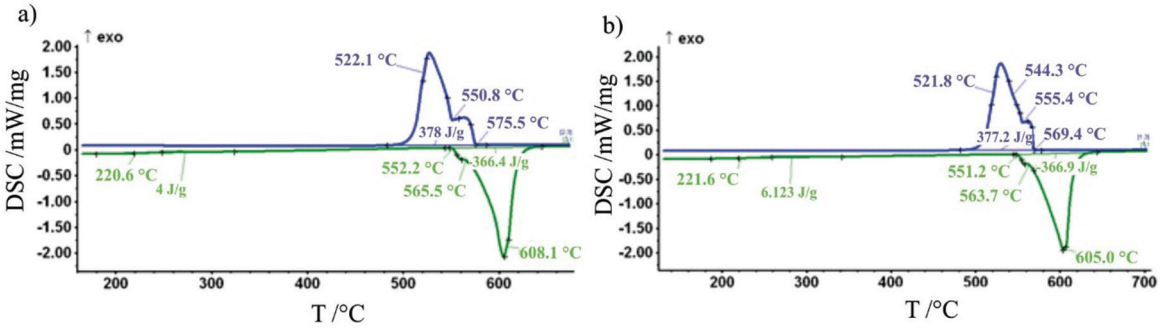

Figure 4: *Heating (green) and cooling (blue) DSC curve of the sample (a) 239 and (b) 239D.*

A light microscope was used to image the microstructure of all samples at various magnifications. Figures 5a and b show the microstructure of sample 239, while Figures 5c and d show sample 239D. According to the literature, the following microstructural components are observed in the microstructures in the figure: primary α-Al dendrites, binary eutectic (α-Al + β-Si), Fe-eutectic phase α-$Al_{15}(Fe,Mn)_3Si_2$ ('Chinese script'), needle shape β-Al_5FeSi phase, and the eutectic phase of Mg_2Si (black) [5]. Due to the presence of magnesium, the formation of the π-$Al_8FeMg_3Si_6$ phase is also possible [12]. Given the presence of strontium in the chemical composition of sample 239, the formation of the Al_2SrSi_2 phase can also be inferred [13]. The black arrows in Figures 5a and c indicate the deleterious β-Al_5FeSi phases, which are hardly observed in the microstructure of sample 239, while they are common in the microstructure of sample 239D. In sample 239, the eutectic (α-Al + β-Si) is much finer and rounder, which is due to the presence of strontium acting as a modifier of the eutectic β-Si.

Figures 6a and b show the microstructures of the as-cast and heat-treated sample 239 (239 and 239T). Figures 6c and d show the microstructures of the cast and heat-treated sample 239D (239D and 239DT). It can be observed that there is a visible decrease in the primary α-Al, according to the literature. A decrease in the eutectic (α-Al + β-Si) is observed especially for sample 239DT. As in the as-cast condition, the density of the β-Al_5FeSi phases in the heat-treated condition is much higher in the secondary alloy (239DT). After heat treatment, the thicker needles are rounded.

Figure 7 shows a comparison of the average hardness values between the qualities of alloys in the as-cast samples and after heat treatment. It can be seen that the hardness of sample 239 increases by ~ 28% and that of 239D alloy increases by ~ 42% after heat treatment. In general, the hardness of the as-cast sample 239D is ~ 6% higher than that of the purer alloy, and after heat treatment it is ~ 24% higher than that of the purer 239 sample.

Figure 8 shows a comparison of tensile test results between qualities of alloy and between the as-cast and heat-treated states. For better quality alloy, tensile strength and yield strength are increased by heat treatment, while elongation is greatly reduced by heat treatment. The alloy produced from secondary raw materials

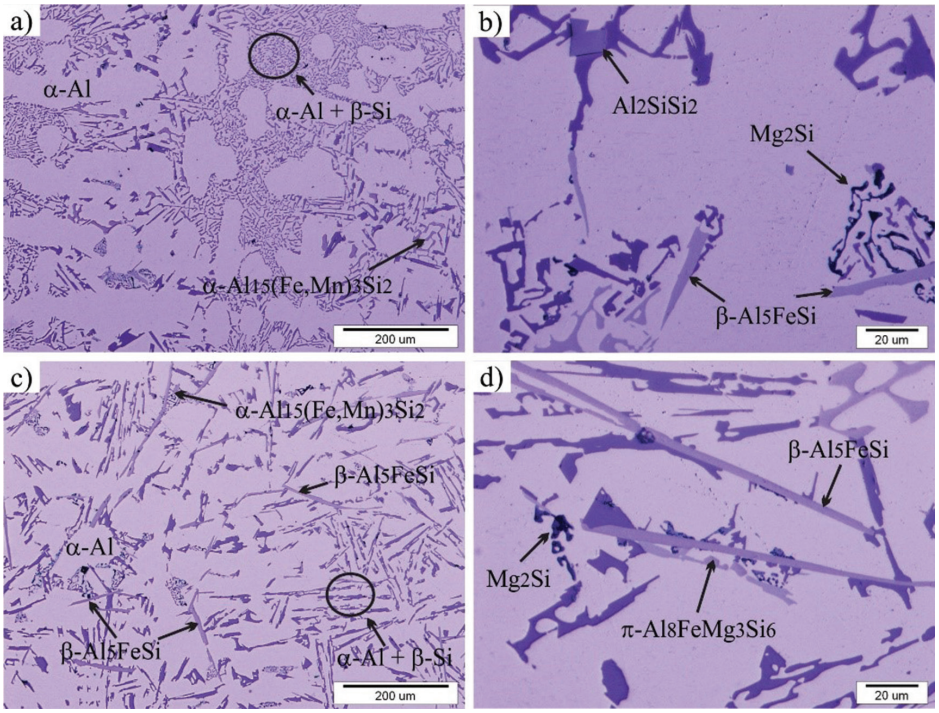

Figure 5: *Micrographs of (a and b) sample 239 and (c and d) sample 239D.*

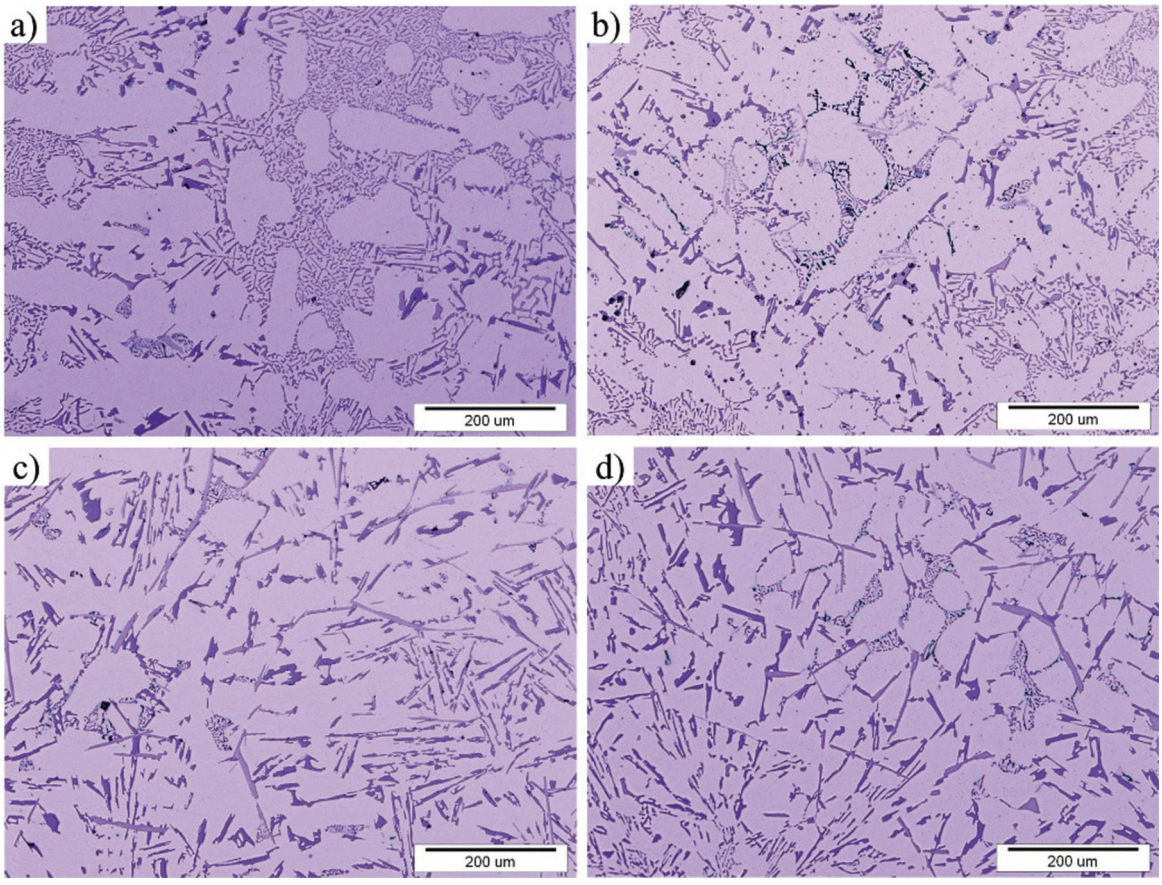

Figure 6: *Micrographs of sample 239 in (a) as-cast state and (b) T6 heat-treated state and of sample 239D (c) in as-cast state and (d) T6 heat-treated state.*

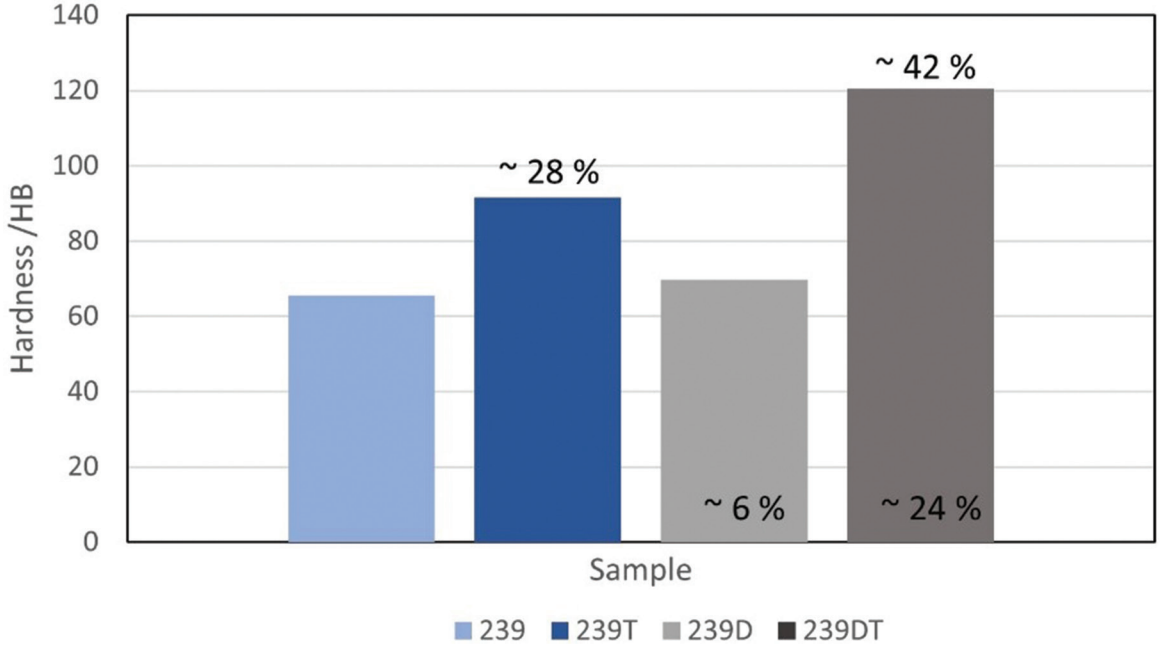

Figure 7: *Hardness of AlSi10Mg alloy and AlSi10Mg(Fe) alloy in as-cast state and after heat treatment.*

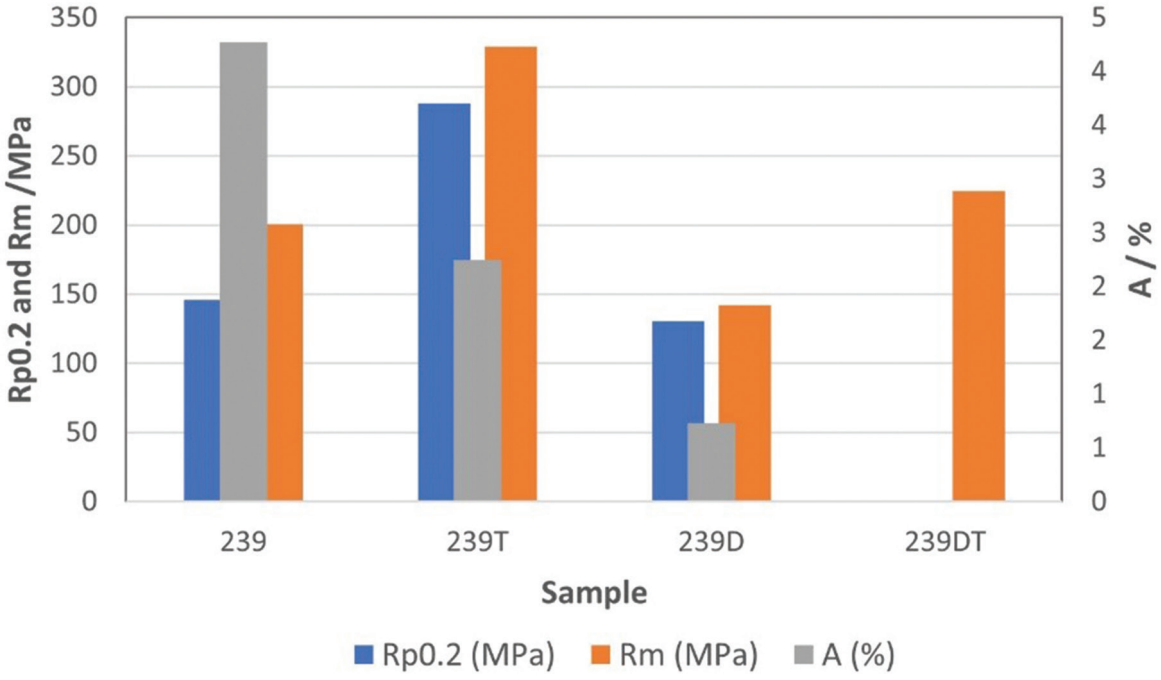

Figure 8: *Tensile test results for 239 alloys and 239D alloys in the as-cast state and after heat treatment.*

has significantly lower mechanical property values in the as-cast condition, and after heat treatment the material was so brittle that the mechanical properties could not be measured.

Conclusion

Thermal analysis methods can give us an important and necessary indication of the quality of the alloys used.

Recycling aluminium is the future from an energy point of view. Therefore, it is important to produce high quality alloys from secondary raw materials that can replace those produced from primary aluminium.

The deleterious β-Al_5FeSi phases were hardly observed in the microstructure of the purer sample, while they are common in the microstructure of inferior quality sample. A visible decrease in the primary α-Al and in the eutectic (α-Al + β-Si) was observed, especially for samples of inferior quality after heat treatment. As in the as-cast condition, the density of the β-Al_5FeSi phases in the heat-treated condition is much higher in the alloy of inferior quality. After heat treatment, the thicker needles are rounded. In general, the hardness of the as-cast sample of inferior quality was ~ 6% higher than that of the purer alloy and after heat treatment was ~ 24% higher than that of the purer sample. For better quality alloy, tensile strength and yield strength are increased by heat treatment, while elongation is greatly reduced by heat treatment. The alloy produced from secondary raw materials has significantly lower mechanical property values in the as-cast condition.

The analysis of the effects of alloy quality of primary and secondary produced AlSi10Mg alloys on solidification, microstructure and mechanical properties revealed significant differences in the results of the analysed properties. Based on the results, we can predict when it is appropriate to use a primary produced alloy with higher purity and when to use a secondary produced alloy with more and higher concentration of alloying elements.

Acknowledgement

The work was co-financed by the Republic of Slovenia, the Ministry of Education, Science and Sport, and the European Regional

Development Fund. The work was carried out in the framework of the project Modelling of Thermomechanical Processing of the Aluminium Alloys for High Quality Products (MARTIN, Grant No.: C3330-18-952012).

References

[1] Yildirim, M., Özyürek, D. (2013): The effects of Mg amount on the microstructure and mechanical properties of Al-Si-Mg alloys. *Materials & Design*, 51, pp. 767-774, DOI:10.1016/j.matdes.2013.04.089.

[2] Kaufman, J.G., Rooy, E.L. (2004): *Aluminium alloy castings: Properties, processes, and aplications*. ASM International, 340 p.

[3] SS-EN 1676:2010. *Aluminium and aluminium alloys - Alloyed ingots for remelting – Specifications* [cited 20/10/2020]. Available on: https://www.stenaaluminium.com/siteassets/document/product-sheets/eng-en-ab-43400.pdf.

[4] Raffmetal the Aluminium Evolution. *Continuous casting alloys: EN AB 43000 AlSi10Mg(Fe) alloy* [cited 11/7/2020]. Available on: https://www.raffmetal.com/web_eng/prodotti.asp?q=1.

[5] Vončina, M., Medved, J., Mrvar, P. (2005): Thermodynamic analysis of MgSi10Mg alloy. *RMZ – Materials and Geoenvironment*, 52(3), pp. 621–633.

[6] Que, Z., Wang, Y., Fan, Z. (2018): Formation of the Fe-containing intermetallic compounds during solidification of Al5Mg2Si0.7Mn1.1 Alloy. *Metallurgical and Materials Transactions A*, 49, pp. 2173–2181, DOI: 10.1007/s11661-018-4591-6.

[7] Ravi, M., Mech, K., Sasidharan, V., et al. (2014): Influence of alloying elements and casting process on the mechanical properties of al-si piston alloy. *National conference on advances in materials and advances in bioprocess engineering. At: Mohandas College of Engineering and technology.*

[8] Girelli, L., Tocci, M., Gelfi, M., Pola, A. (2019): Study of heat treatment parameters for additively manufactured AlSi10Mg in comparison with corresponding cast alloy. *Materials Science & Engineering A,* 739, pp. 317–328, DOI: 10.1016/j.msea.2018.10.026.

[9] Zyguła, K., Nosek, B., Pasowiec, H., Szysiak, N. (2018): Mechanical properties and microstructure of AlSi10Mg alloy obtained by casting and SLM technique. *World Scientific News*, 104, pp. 462–472, DOI: 10.1007/s12633-021-01340-9.

[10] Bäckerud, L., Chai, G., Tamminen, J. (1990): *Solidification characteristics of aluminium alloys. Volume 2, foundry alloys.* AFS/SKANALUMINIUM: Stockholm, 266 p.

[11] Medved, J., Kores, S., Balaško, T., Vončina, M. (2019): Influence of minor alloying element addition on aluminium casting alloys, *Livarski vestnik,* 66(3), pp. 191-202.

[12] Vončina, M., Medved, J., Kores, S., Xie, P., Schumacher, P., Li, J. (2013): Precipitation microstructure in Al-Si-Mg-Mn alloy with Zr additions. *Materials characterization*, 155, 8 p., DOI: 10.1016/j.matchar.2019.109820.

[13] Petrič, M. (2013): *Sprememba dimenzij in električne upornosti med strjevanjem litin iz sistema Al-Si.* Ph. D. Thesis. University of Ljubljana, Faculty of Natural Sciences and Engineering, Department of Materials and Metallurgy: Ljubljana, 138 p.